Hindawi
Science and Technology of Nuclear Installations
Volume 2017, Article ID 3497103, 10 pages
https://doi.org/10.1155/2017/3497103

Research Article

Heat Transfer Analysis of Passive Residual Heat Removal Heat Exchanger under Tube outside Boiling Condition

Yanbin Liu, Xuesheng Wang, Qiming Men, Xiangyu Meng, and Qing Zhang

School of Mechanical and Power Engineering, East China University of Science and Technology, Room 637, Building 17, 130 Meilong Road, Shanghai 200237, China

Correspondence should be addressed to Xuesheng Wang; wangxs@ecust.edu.cn

Received 11 July 2016; Revised 19 October 2016; Accepted 26 January 2017; Published 6 March 2017

Academic Editor: Eugenijus Uščuras

Copyright © 2017 Yanbin Liu et al. This is an open access article distributed under the Creative Commons Attribution License, which permits unrestricted use, distribution, and reproduction in any medium, provided the original work is properly cited.

The Passive Residual Heat Removal Heat Exchanger (PRHR HX) is an important part of the Passive Residual Heat Removal System (PRHRS). The C-shaped bundle is being used in the PRHR HX. A test facility of C-shaped tube immerged in a water tank was built to research the heat transfer of the PRHR HX. Through the experiments, three regions were found within a particular period of time during the heating process in the tank: natural convection region, transition region, and saturation boiling region. For the tube outside saturation boiling, comparisons of three different correlations in literatures with the experimental data were carried out. Results show that the Rohsenow correlation provides a best-estimate fit with the experimental results. For the tube outside transition region, a formulation is put forward to reduce error based on the Rohsenow subcooled boiling correlation.

1. Introduction

AP600 and AP1000 are based on proven Westinghouse PWR technology that has been successfully operated in hundreds of reactor-years of operation. AP1000 is an updated version of the AP600; both AP600 and AP1000 have the same passive safety-related systems which include the passive core cooling system (PXS) [1]. A key feature of the passive core cooling system is the Passive Residual Heat Removal Heat Exchanger (PRHR HX) that provides decay heat removal for postulated LOCA and non-LOCA events. The PRHR HX is a C-tube heat exchanger located in the in-containment refueling water storage tank (IRWST) above the core promoting natural circulation heat removal between the reactor cooling system and the tank [2].

The main heat transfer mechanisms through the tubes are single phase natural (possibly, forced) convection on the inside of the tubes, conduction through tube material, and, finally, subcooled/saturated nucleate pool boiling on the outside of the tubes [3].

Several correlations were proposed in literatures to predict the heat transfer coefficients under convection and boiling conditions, such as the Lienhard [4], Gnielinski [5], and Petukhov [6] single phase forced convection correlations. Natural convection heat transfer coefficients of tube outer surface correlations have been proposed in past years; Langmuir and Churchill-Chu Correlations [7], McAdams Correlations [8], and MARS Code Correlations [9] were frequently used. Jens-Lottes correlation [10], Rohsenow Correlation [11], and Corletti Correlation [12] have been proposed in related articles for calculating saturation boiling heat transfer.

There are several published research articles about PRHR HX; Kang [3] performed an experimental parametric study of a tubular heat exchanger under nucleate pool boiling conditions. With different test parameters of tube diameter, surface roughness, and tube length, a new empirical heat transfer correlation was obtained. In his study the tubes used was vertical, not C-shaped tubes. Yonomoto et al. [10] analyzed the heat transfer performance of the PRHR during integral experiments that simulated small-break LOCAs in the AP600 reactor and predicted the total heat transfer rate by using correlations available in literature. The reason why he used the correlations was not given. Pan [13] conducted a numerical study of AP600 PRHR HX with FLUENT and obtained the temperature distribution of IRWST at different times. The transient numerical results show that the heat transfer performance of the PRHR HX and IRWST is consistent with AP600 experimental results. Xue et al. [14]

conducted a non-steady-state numerical simulation of shell-side of AP1000 PRHR HX by employing fluent software, got the visual information of temperature field and flow field, and studied its heat transfer and flow characteristics. Li et al. [15] investigated the pool boiling heat transfer characteristics of smooth tube and a machined porous surface tube by using high-pressure steam condensing inside the tube as heating source. Jia et al. [16] simulated Passive Residual Heat Removal System (PRHRS) with different numbers of C-type heat transfer tubes and different coolant inlet temperatures via FLUENT software. Xia et al. [17] proposed two schemes in order to improve the heat transfer effect of PRHR HX. First, lengthen the horizontal section and shorten the vertical section. Second, flat layout replaces centralized layout. These models were established and simulated by FLUENT. Heat transfer coefficients of C-tubes were comparatively analyzed to study which kind of the heat transfer effect was better. Zhang et al. [18] performed a three-dimensional (3D) simulation on the localized thermal hydraulic characteristics in the IRWST side of the AP1000 Passive Residual Heat Removal System in the study. The simulation employs the porous media model to simplify the complicated tube bundle structure. Men et al. [19] analyzed the tube inside and outside heat transfer mechanism of PRHR HX under natural convection condition, and the results were compared with simulated results of the single-tube coupling model three-dimensional natural circulation in the IRWST. In the work, the theoretical calculation method is suitable for the heat transfer calculation of PRHR HX. Zhang et al. [20] simulated the transient single phase heat transfer behavior of PRHR HX model in the benchmark test condition. The calculated results were compared with the experimental data and empirical correlations, and there were some deviations. Men et al. [21] researched the applicability of different heat transfer correlations for the PRHR HX design and investigated the mixing characteristics in the IRWST. All the results in his paper are obtained under the condition of natural convection on the tube outer surface. Boiling on the tube outer surface was not considered. Wang et al. [22] analyzed the influence of tube bundle structure on the performance of PRHR HX. The results show that, in the region of single phase natural convection and mild boiling, the transfer coefficient of triangle bundle arrangement is superior to the existing design. Li et al. [23] carried out a heat transfer experiment of PRHR HX with three C-type tubes. And through numerical calculation, the correlations for calculating the subcooled heat transfer of the outside of the tube were obtained. Results are in good agreement with the experimental data. Lu et al. [24] investigated the natural convection and heat transfer behavior of the C-shape heating rods bundle used in PRHR HX based on an overall scaled IRWST and PRHR HX test bench. Both the overall and local hydraulic performance of the IRWST and PRHR HX models are analyzed. Huang et al. [25] developed an analysis tool based on the drift flux mixture flow model to evaluate the reliability of the water cooling PRHRS, but further validation of the analysis tool is needed before it is used in the design and safety analysis of the water cooling PRHRS.

Because, in literature [21], the mixing characteristics in the IRWST and the heat transfer calculation of the PRHR HX under the condition of natural convection on the tube outer surface were deeply studied through experiments, the main purpose of this study is to research the mixing characteristic in the IRWST from natural convection to boiling condition, find out the best fit one from several commonly used correlations for PRHR HX saturation boiling heat transfer calculation, and try to come up with a new formula to improve calculation accuracy for the tube outside subcooled boiling.

Table 1: Parameters of experimental facility.

Parameters	Value
Tank diameter	600 mm
Tank height	1500 mm
C-shaped tube outside diameter	19.05 mm
C-shaped tube thickness	1.65 mm
C-shaped tube length in vertical direction	1200 mm
C-shaped tube length in horizontal direction	450 mm
Heat power	16 kW

2. Experimental Setup

In Figure 1 was a new PRHR HX experimental system. Some modifications were made on the experimental setup in literature [21]. It mainly consisted of a cylinder pressure vessel, two electric heating jackets, a water tank, a C-shaped tube, some wall and liquid thermocouples, and a centrifugal pump. The IRWST was made by a cylindrical tank filled with water at atmospheric pressure and filled to a level 0.1 m above the top of the heat exchanger tube. Two view ports were installed on both sides of the tank for visual observation. The material of the pressure vessel, the water tank, and the C-tube was 304 stainless steel. The parameters of experimental facility were summarized in Table 1.

A cover with heat exchanging function which was used to simulate the actual situation was installed on the top to cooling the steam generated in the tank. The cooling medium was water. A filter was installed to ensure the cleanliness of fluid inside the tube. An expansion joint was installed at the pump outlet to reduce the pipeline vibration. A pressure gauge and a relief valve were installed on the top of the pressure vessel to monitor the pressure and provide overpressure protection. The influence of separation plate and Automatic Depressurization System (ADS) 1–3 sparger in IRWST was also ignored in this experiment.

The fluid inside tube was heated by 2 electric heating jackets rated at 8 kW. Two Pt100 thermocouples were installed in different areas of the pressure vessel and worked with two temperature controllers to regulate the fluid temperature in pressure vessel. The flow rate in tube was measured by a turbine flow meter. Electrical signals from the transducers were processed by a data acquisition system.

As shown in Figure 2, there were 10 sheath thermocouples inserted in the heat exchanger tube, 2 of which were installed at each end of the tube to measure the inlet and outlet

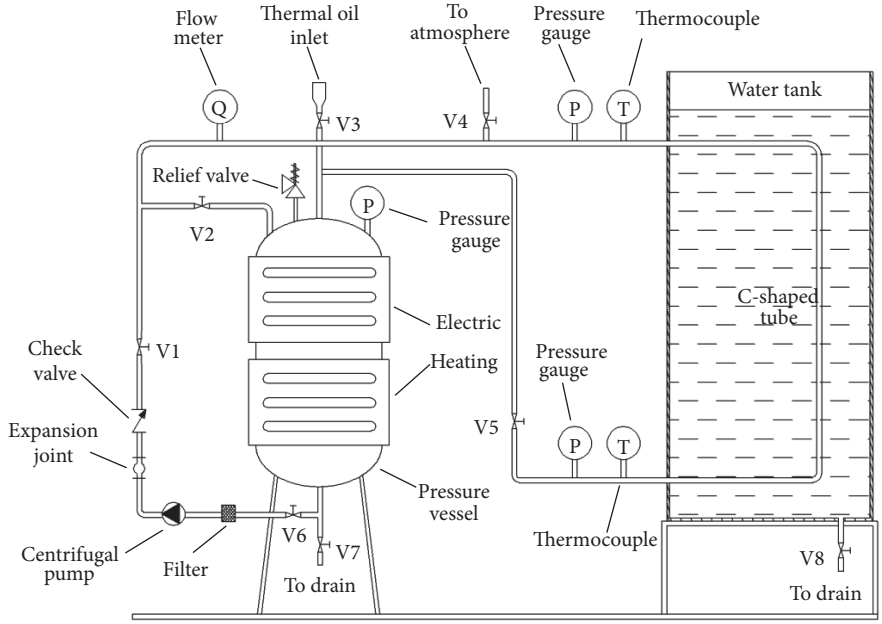

Figure 1: Experimental apparatus diagram.

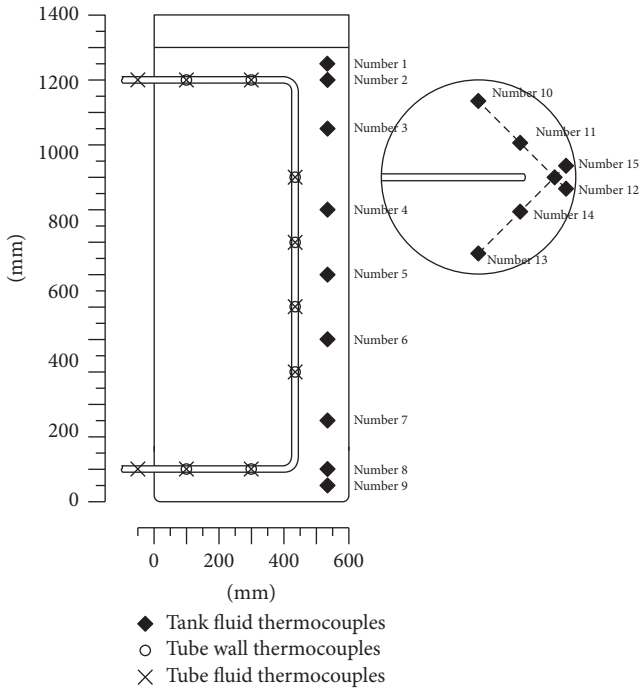

Figure 2: Water tank and thermocouple layout.

fluid temperatures. Four wall thermocouples were welded on each position of the tube outer surface to get an average wall temperature. Six tank water thermocouples were in 2 equal groups, located at two different positions along vertical direction of the tank. The group number 10~12 is higher than the group number 13~15. The arithmetic mean of the 3 thermocouples in each group was used as the average tank fluid temperature of the corresponding elevation. Number 1~9 thermocouples were installed in a line along the vertical direction.

Table 2: Uncertainties of measured parameters.

Parameters	Uncertainties
Thermal oil temperature	±0.61°C
Tube outside wall temperature	±0.42°C
Tank water temperature	±0.41°C
Thermal oil flow rate	±0.5%
Heat transfer capacity	±5.52%
Heat transfer coefficient	±4.38%

Instruments were calibrated and the uncertainty of measured parameters was evaluated according to the procedure suggested by Abernethy and Thompson [26]. The results were summarized in Table 2.

In the experiment, the fluid inside tube was thermal oil, and the fluid used in tank was distilled water. Considering the applicability under different conditions, L-QB320 thermal oil was chosen here, and it was often used below 573 K. In order to ensure the accuracy of the calculation, the viscosity and thermal conductivity of L-QB320 were fitted according to temperature. Specific heat capacity does not change with temperature obviously. Table 3 was physical parameters of L-QB320.

Using thermal oil as heating medium can gain high temperature under low operating pressure and also obtain high tube wall temperature, so the supercooling degree was higher than using steam. Although the viscosity of thermal

Table 3: Physical parameters of L-QB320.

Parameters	Value
Viscosity (Pa·s)	$0.14548 \times \exp(-t/37.1453) + 0.00206$
Thermal conductivity (W/m·°C)	$0.14307 - 1.48343 \times 10^{-4} t$
Specific heat (J/kg·°C)	709

oil was higher, the heat transfer outside tube was closer to that under actual condition.

The operating procedure of the experiments was as follows: first, fill the tank and tube loop with fluids; second, remove dissolved gasses in fluids; third, heat up pressure vessel; fourth, start the test; last, record experimental data.

Thermal oil was transported to C-tube by the pump, heating the water in tank. Because flow state inside tube had no relation with driving force and was decided by Reynolds number, using forced convection instead of natural convection was reasonable. In order to easily regulate main flow rate, a bypass tube was added from bottom to top of the pressure vessel.

3. Experimental Conditions and Data Reduction

The primary data measured in the experiment included tube flow rates, tube fluid axial temperature distribution, tube outside wall temperatures, and tank fluid temperatures.

Combining the pump capacity, the heating temperature was set at 493 K which was the highest affordability of the pump to obtain tube outside boiling condition. When the heating temperature reached 493 K and opened the heating loop and the temperature in vessel gradually decreased to 393 K with the heat exchanging, then it began to rise. It finally kept stable at 433 K when the water in tank had already been saturated boiling. It was reasonable that the electric heating power kept stable because the PRHR HX was used at small-break loss-of-coolant accidents in the reactor.

In the experiment, the main valve was kept fully open and the bypass was cut off to obtain high Reynolds number. Experiment goes on from thermal oil entering the main loop to water in tank reaching saturated boiling. The determined test conditions were summarized in Table 4.

Several tests were conducted under the conditions in Table 4. According to the tank water temperature changes, the maximum error is about 13.34%.

Experiment process was unsteady. Using steady calculating method to handle primary data was unsuitable. The heat exchange tube was virtually divided into 11 cells along the longitudinal direction of the tube, 3 cells for the upper horizontal section, 5 for the vertical section, and 3 for the lower horizontal section.

The calculating method was similar to the method mentioned by Men et al. [21], but the difference between tube inside bulk fluid temperature and centerline temperature was ignored in this research because the measured centerline temperature was approximately equal to the bulk temperature which has been proved by Men et al. [21]. Thus here use measured tube inside temperature as the bulk fluid temperature. The program used raw test data to calculate the wall heat flux, inside wall temperature, and heat transfer coefficients on both sides of C-tube and compared the measured heat transfer with the heat transfer coefficients predicted by several selected correlations.

4. Results and Discussion

Figure 3 is tank fluid temperatures distribution in the vertical direction as a function of time; with time going on, the elevations at the top of the tank are shown to heat up to saturation temperature firstly, and the lower elevations are delayed. When upper water reaches saturation temperature (12065 s, 373.22 K), lower water temperature is 313.21 K, when experimental time is 15525 s, lower water temperature reaches saturation temperature.

Figure 4 is number 10~12 and number 13~15 thermocouples temperature distribution, which shows that the difference between each of the two temperatures of the 3 positions at the same elevation is within 1 K. The small range of temperatures indicates that the tank water was well mixed at each elevation.

Several representative times were chosen to analyze the rule of heat transfer in heat sink by way of dividing heat transfer cells in previous section. The temperatures of the outer wall of heat exchanger tube and the water tank along the tube at different times are shown in Figure 5.

The outer wall temperature of each cell along the tube and the tank fluid temperature at the same elevation are shown in the Figure at 300 seconds, 6500 seconds, 12100 seconds, and 14200 seconds. Because the temperature measuring points of the tank and the outer wall of the tube were staggered, the tank fluid temperatures at the corresponding positions of the outer wall were calculated by using liner interpolation.

Figure 5(a) shows the temperatures of the tube outer wall and the tank fluid at 300 seconds. At the initial heating period, the temperature of thermal oil inside the tube was high, but the tank fluid temperature was low (the top of the tank is 298.19 K). Thus the temperature of the tube outer wall was low and did not reach saturation temperature of the fluid (373.15 K). After a short period of heating, the top of tank temperature rose firstly and the outer wall temperature of the cells in horizontal section rose over saturation temperature while the tank fluid temperature did not reach it. Condensate depression existed between the wall and the fluid. Heat transfer mechanism at that time was different from that in initial heating period.

As seen in Figure 5(b), the wall temperatures of the cells in horizontal section, respectively, reach 373.46 K and 373.35 K at 6500 seconds. The temperature of the tank fluid at corresponding location is 358.24 K. Heat transfer at the location was different from that in initial heating period but the same with the form of heat transfer in transition region. It was seemingly the heat transfer form of subcooled boiling.

With the analysis of the temperature at 12100 seconds (see Figure 5(c)), it can be found that along the heat transfer tube, there is such a region that the temperatures of the outer wall

Table 4: Summary of test conditions.

Duration (s)	Inlet temperature (K)	Mass flow rate (kg/s)	Tank fluid initial temperature (K)	Tank fluid level (m)
16585	395.78~425.42	0.85	283.47	1.4

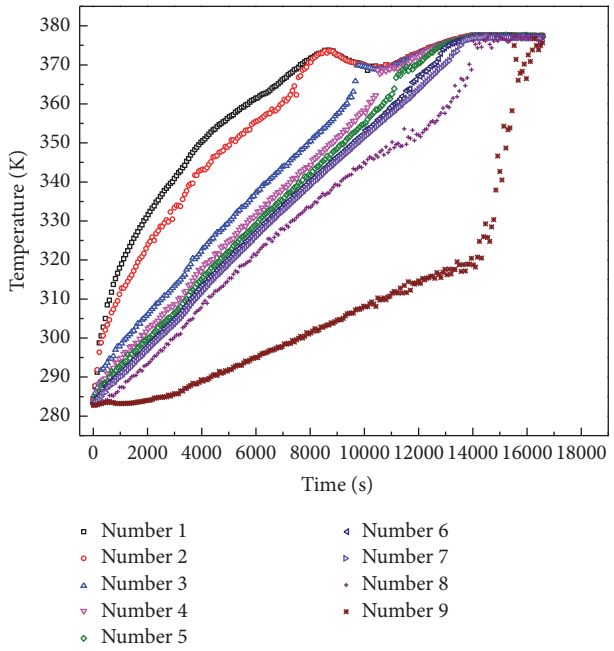

Figure 3: Temperature distribution in the vertical direction of the water tank.

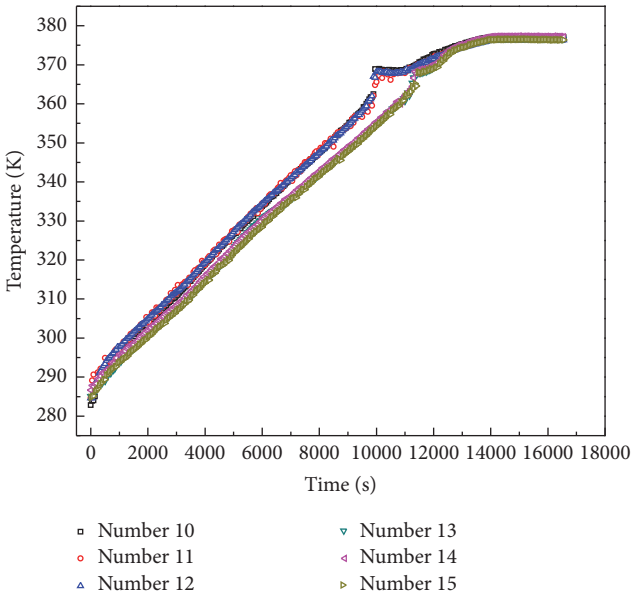

Figure 4: Temperature distribution in the horizontal direction of the water tank.

and the fluid are both higher than saturation temperature. There is also a region that the wall temperature is higher but the fluid temperature is lower than saturation temperature. What is more, in the last two cells which are in the lower horizontal section, the temperatures of both the outer wall and the fluid are lower than saturation temperature. It is the time that three heat transfer forms coexist. At 13000 seconds (see Figure 5(d)), all measured outer wall temperatures rise over saturation temperature. At the moment, natural convection region does not exist. At 14200 seconds (see Figure 5(e)), all the temperatures of the outer wall and the fluid are both higher than saturation temperature.

The analysis above indicates that the heat transfer form in the water tank is as follows: at initial period, natural convection happens in the whole water tank. With the heating process going on, the outer wall temperature of C-shaped tube in horizontal section in the top of the tank reaches saturation temperature while the bulk temperature is still low. The form of heat transfer at the top of the tank is neither saturation boiling nor natural convection. Natural convection exists at the bottom of the tank where the temperature of the outer wall does not reach saturation temperature. When the bulk temperature of the tank top reaches saturation temperature, saturation boiling heat transfer exists in the tank top and natural convection exists in the bottom of the tank. There is a transition region in between the top and bottom of the tank; the transition region moves towards the bottom of the tank with the heating process until all tank water becomes saturation boiling.

It can be concluded that, in the heating process, there are virtually two forms of heat transfer, saturation boiling and natural convection, and also a third form which is predicated as subcooled boiling heat transfer that is different from the former two in presentation. At a certain time of the heating process, there are three heat transfer regions in the water tank: saturation boiling region, transition region, and natural convection region, which are shown in Figure 6.

For tube outside natural convection region, in literature [21], comparisons of different correlations with the experimental data were made and the McAdams correlations for both horizontal and vertical regions are best-estimated. The average errors are about 0.55% for horizontal region and about 3.28% for vertical region.

McAdams correlation for horizontal section is as follows:

$$\mathrm{Nu} = 0.53\,(\mathrm{Gr}\cdot\mathrm{Pr})^{1/4}. \quad (1)$$

McAdams correlation for vertical section is as follows:

$$\mathrm{Nu} = 0.13\,(\mathrm{Gr}\cdot\mathrm{Pr})^{1/3} \quad \left(\mathrm{Gr}\cdot\mathrm{Pr} > 10^{9}\right). \quad (2)$$

Here Nu, Gr, and Pr represent Nusselt number, Grashof number, and Prandtl number of tube outside fluid.

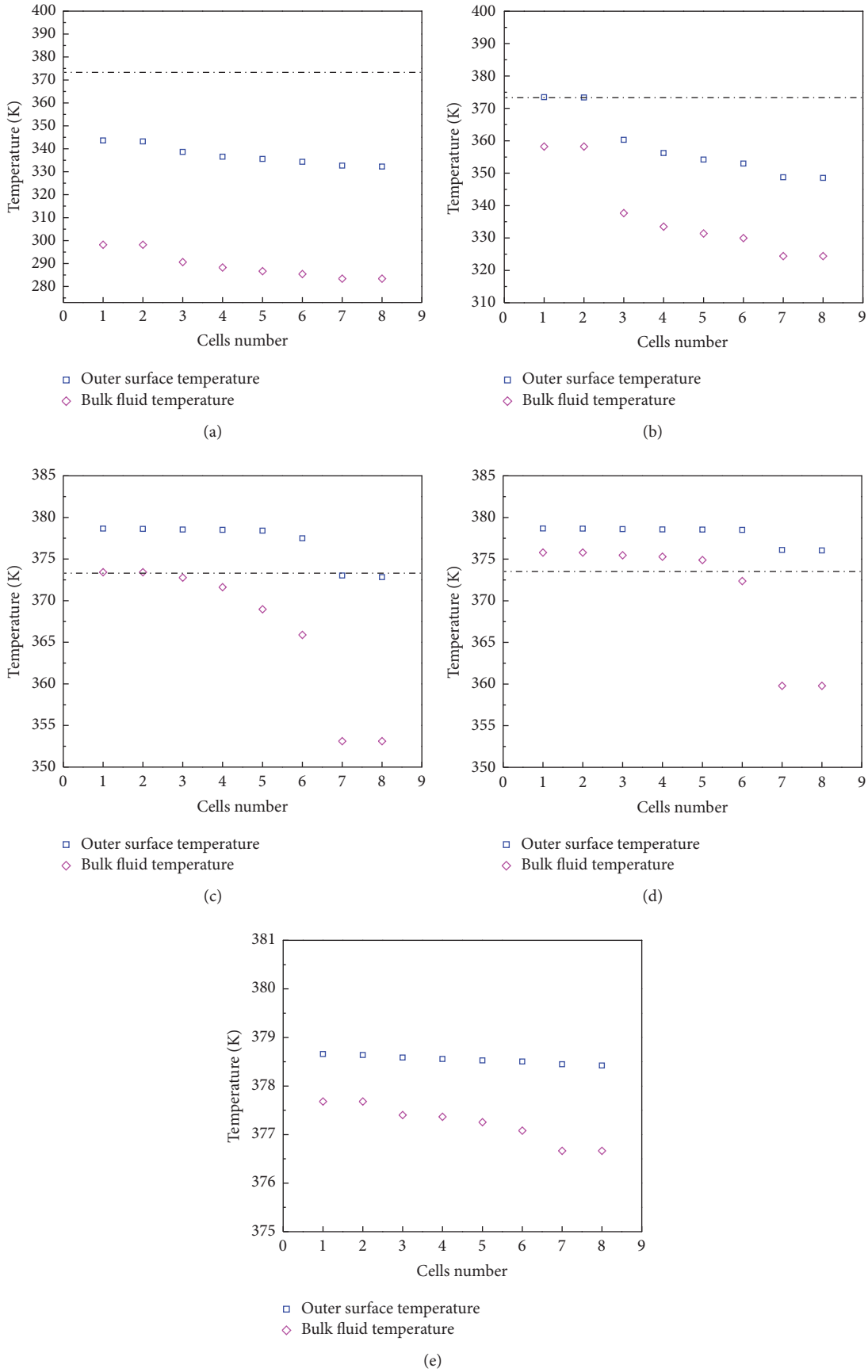

Figure 5: Tube outer surface and tank fluid temperature distribution at different times. (Here the cells number was divided by using tube wall thermocouples position as cells center.) (a) 300 s; (b) 6500 s; (c) 12100 s; (d) 13000 s; (e) 14200 s.

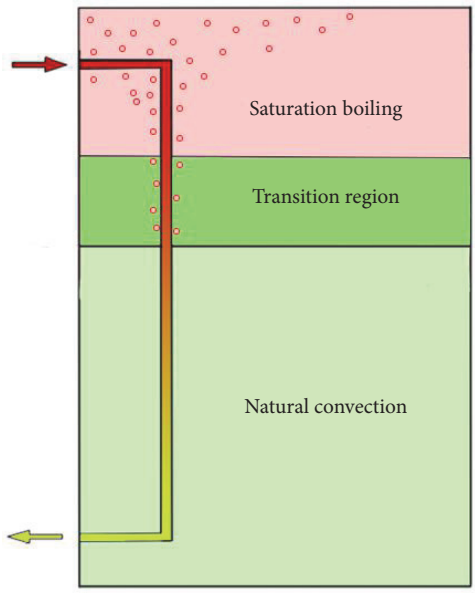

Figure 6: Schematic diagram of heat transfer mechanism.

For saturation boiling region, many empirical correlations have been proposed in related literatures, including Jens-Lottes correlation, Rohsenow Correlation, and Corletti correlation. They are different in form and scope of application. It is necessary to find out the more suitable correlation for boiling heat transfer calculation outer PRHR HX tube. Four times after the water in the tank reached saturated boiling were chosen to calculate related data according to empirical correlations.

4.1. Jens-Lottes Correlation [10]

$$h = \Delta T^3 \left[1.22e^{(1.619\times10^{-7}p)}\right]^4; \quad (3)$$

here h is heat transfer coefficient, W/(m^2·K), ΔT is the temperature difference of the tank wall when it is in normal temperature and in saturation temperature, K, and p is pressure, Pa.

4.2. Rohsenow Correlation [11]

$$\frac{c_{pf}\left(T_w - T_{\text{sat}}\right)}{h_{fg}} = C_{sf}\left[\frac{q}{\mu_f h_{fg}}\sqrt{\frac{\sigma}{g\left(\rho_l - \rho_v\right)}}\right]^{0.33}\left(\frac{c_{pf}\mu_f}{k_f}\right)^m; \quad (4)$$

here c_{pf} is specific heat at constant pressure of saturated liquid, J/(kg·K), h_{fg} is latent heat of vaporization of water, J/kg, T_w is the temperature of the outer wall of heat exchange pipe, K, T_{sat} is saturation temperature of the medium, K, C_{sf} is the empirical coefficient of the superface of solid or liquid combination, we take it as 0.013 in this calculation, q is boiling heat flux, W/m^2, μ_f is dynamic viscosity of saturated liquid, Pa·s, σ is surface tension of the interface of the liquid and vapor, N/m, ρ_l is the density of saturated liquid, kg/m^3, ρ_v is the density of saturated vapor, kg/m^3, k_f is thermal conductivity of saturated liquid, W/(m·K), m is empirical index, and we take m as 1.0 since the medium is water in the experiment.

4.3. Corletti Correlation [12]

$$q = \mu_f h_{fg}\left[\frac{g\left(\rho_f - \rho_g\right)}{g\sigma}\right]^{1/2}\left(\frac{c_{pf}\left(T_w - T_{\text{sat}}\right)}{h_{fg}\text{Pr}_f C_{sf}}\right)^3. \quad (5)$$

Corletti correlation has modified Rohsenow correlation on the basis of experimental data. In Corletti correlation, $C_{sf} = 0.034$. Other parameters in both the two correlations are the same in method of taking value.

Figures 7(a)–7(d) show the comparison of the actual data of heat flux in each cell of heat exchange tube at four different times when the water in the tank reaches saturated boiling and the data calculated according to those empirical correlations. Cells 1-2 and cells 6-7 are in the upper and the lower horizontal section; cells 3–5 are in the vertical section. We can visually observe that, among the three data items according to the empirical correlation, the data of Rohsenow correlation has the minimum error while the data of Corletti correlation has the maximum error with the experimental data. At the time of 15000 s the maximum errors of the two correlations with the experimental data are separately 5.19% and 94.83%, and the maximum error of Jens-Lottes correlation with experimental data is 12.68%. The data at the other three times are similar with those at 15000 s. The maximum errors are 12.78%, 95.29%, and 19.73% in turn; all of them appear at the time of 16500 s. The average error of Rohsenow correlation is about 8.37%.

According to the figures, the Rohsenow correlation is most approximate to the experimental data. While that Corletti correlation has the maximum errors with the experimental data, which reaches 90%, the reason for the errors may be that the experimental conditions are greatly different. In [3], it is mentioned that "for example, the heat flux values calculated by the generalized PRHR boiling correlation of Corletti et al. (1990) are less than one-tenth of the value predicted by Rohsenow (1952) correlation. One of the possible reasons for the discrepancy can be explained by the effect of the orientation of heated surface." In addition, the Corletti boiling correlation is modified based on Rohsenow correlation through experiments. Modified correlation may be sensitive to different experimental conditions and does not have universal applicability.

For the transition region, published heat transfer calculating research literatures are few. In literature [27], a correlation was recommended

$$\frac{Q}{A} = h_b\left(T_w - T_{\text{sat}}\right) + h_n\left(T_w - T_f\right); \quad (6)$$

here Q/A is heat flux, W/m^2, T_w is the temperature of the outer wall of heat exchange pipe, K, T_{sat} is saturation temperature of the medium, K, T_f is tank fluid temperature, h_n is heat

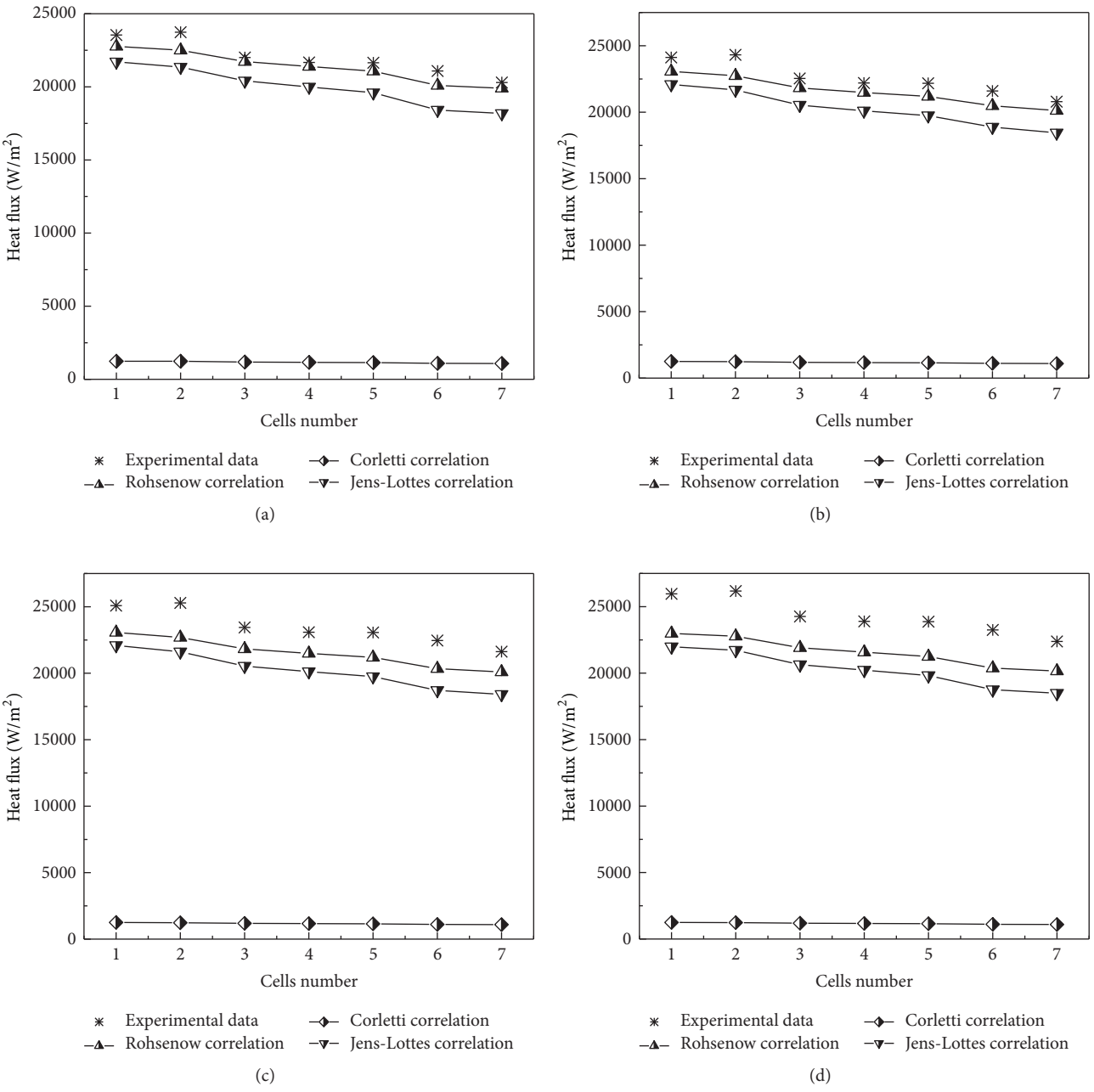

Figure 7: Comparison of heat flux at different times. (Here the cells number was divided by using tube wall thermocouples position as cells boundary.) (a) 15000 s; (b) 15500 s; (c) 16000 s; (d) 16500 s.

transfer coefficient before nucleate boiling, W/(m^2·K), and h_b is saturation boiling heat transfer coefficient, W/(m^2·K).

According to the temperature distribution, at 12100 s, three heat transfer regions coexist. Choose the data at this time and calculate heat flux and wall superheat. Here the correlations used are McAdams correlations and Rohsenow correlation. Figures 8(a) and 8(b) are the comparison of heat flux in horizontal and vertical cells.

In Figure 8(a), the maximum heat flux errors of the two correlations with the experimental results are separately 5.24% and 5.83%. The McAdams correlation and Rohsenow saturation boiling correlation are verified applicable again to calculate the natural convection and saturation boiling condition separately.

In Figure 8(b), the experimental data of vertical cells has some distance to the two curves. It shows that the McAdams correlation and Rohsenow saturation boiling correlation are not applicable to calculate the heat transfer. But the maximum error between the Rohsenow subcooled boiling correlation and the experimental result is 8.49%.

The errors between experimental results and the Rohsenow subcooled boiling correlation are probably caused by

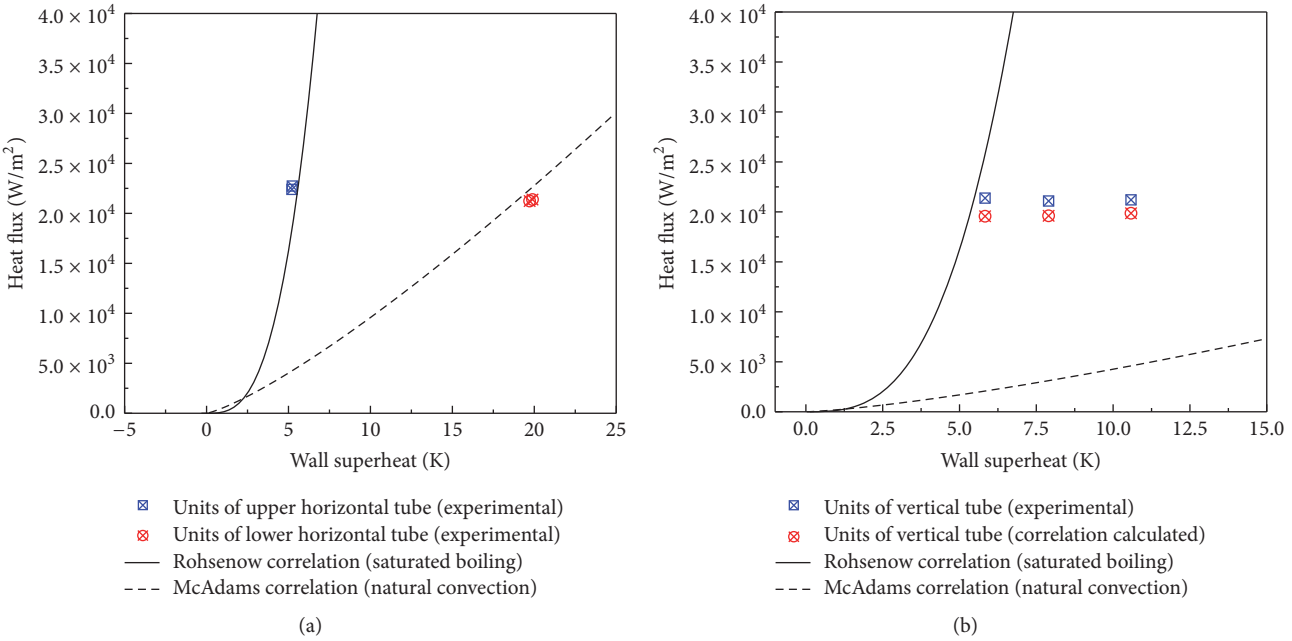

FIGURE 8: Comparison of experimental heat flux with the experience formulation at 12100 s. (a) Comparison of heat flux in horizontal cells. (b) Comparison of heat flux in vertical cells.

the different experimental conditions. In this experiment, three heat transfer regions coexist, but the Rohsenow subcooled boiling correlation was proposed based on simple subcooled boiling condition. In formula (6), the subcooled boiling heat flux can be gotten by simply adding the saturation boiling heat flux and the natural convection heat flux under the same temperature difference together. Through further analysis with the comparison results, it can be found that the calculated results from formula (6) are more accurate when natural convection is playing a main role in heat transfer process, and also the smaller the supercooling degree is, the bigger the error is, which apparently is not reasonable. In order to reduce error, it is necessary to come up with a formulation.

The formulation form adopted here is as follows, to revise the Rohsenow subcooled boiling correlation

$$q_{\text{sub}} = C_1 q_b + C_2 q_n. \tag{7}$$

Here q_{sub} is subcooled boiling heat flux, W/m^2, q_b is saturation boiling heat flux, calculated by formula (4), W/m^2, q_n is natural convection heat flux, calculated by formulas (1) and (2), W/m^2, and C_1 and C_2 are correction factors.

After 6500 s, take wall temperatures and tank water temperatures every other 500 s, and calculate the transition region heat flux. Use the Origin software to do user-defined multivariable nonlinear fitting, and the result is as follows:

$$q_{\text{sub}} = 1.077 \cdot q_b + 0.893 \cdot q_n. \tag{8}$$

Here the fitting errors of C_1 and C_2 are separately 3.02% and 3.24%. According to the experimental condition, the application scope of formula (8) is as follows:

$$\begin{aligned} &T_w > T_{\text{sat}} \\ \text{or } &T_w = T_{\text{sat}}, \\ &T_f < T_{\text{sat}}, \\ &0^\circ\text{C} < T_w\text{-}T_f < 23.8^\circ\text{C}. \end{aligned} \tag{9}$$

See, from formula (8), the proportion of natural convection heat flux value which is reduced and the proportion of saturation boiling heat flux value which is increased.

5. Conclusions

(1) The tank water temperatures increase with the rise of elevation in the vertical direction, while the temperatures keep nearly uniform in the horizontal directions.

(2) At a certain time of the heating process, there are three heat transfer regions in the water tank: natural convection region, transition region, and saturation boiling region.

(3) There are five states with temperature rising: natural convection; natural convection and transition boiling; natural convection, transition boiling, and saturation boiling; transition boiling and saturation boiling; saturation boiling.

(4) The Rohsenow correlation is more acceptable than the Corletti correlation and Jens-Lottes correlation for tube outside saturation boiling heat transfer calculation.

(5) For the transition region, based on the Rohsenow subcooled boiling correlation and experimental data, a new formula is proposed to improve calculation accuracy.

Competing Interests

The authors declare that they have no competing interests.

References

[1] T. L. Schulz, "Westinghouse AP1000 advanced passive plant," *Nuclear Engineering and Design*, vol. 236, no. 14-16, pp. 1547–1557, 2006.

[2] R. F. Wright, J. R. Schwall, C. Taylor, N. U. Karim, J. G. Thakkar, and T. Schulz, "AP1000 passive residual heat removal heat exchanger confirmatory analysis," in *Proceedings of the Fourteenth International Conference on Nuclear Engineering (ICONE '06)*, Nuclear Engineering Division, Miami, Fla, USA, July 2006.

[3] M.-G. Kang, "Experimental investigation of tube length effect on nucleate pool boiling heat transfer," *Annals of Nuclear Energy*, vol. 25, no. 4-5, pp. 295–304, 1998.

[4] J. H. Lienhard, *A Heat Transfer Textbook*, Phlogiston Press, Cambridge, Mass, USA, 3rd edition, 2008.

[5] V. Gnielinski, "New equations for heat and mass transfer in turbulent pipe and channel flow," *International Journal of Chemical Engineering*, vol. 16, no. 2, pp. 359–368, 1976.

[6] B. S. Petukhov, "Heat transfer and friction in turbulent pipe flow with variable properties," *Advances in Heat Transfer*, vol. 6, pp. 503–564, 1970.

[7] S. W. Churchill and H. H. S. Chu, "Correlating equations for laminar and turbulent free convection from a vertical plate," *International Journal of Heat and Mass Transfer*, vol. 18, no. 11, pp. 1323–1329, 1975.

[8] W. H. McAdams, *Heat Transmission*, McGraw-Hill, New York, NY, USA, 3rd edition, 1954.

[9] J.-J. Jeong, K. S. Ha, B. D. Chung, and W. J. Lee, "Development of a multi-dimensional thermal-hydraulic system code, MARS 1.3.1," *Annals of Nuclear Energy*, vol. 26, no. 18, pp. 1611–1642, 1999.

[10] T. Yonomoto, Y. Kukita, and R. R. Schultz, "Heat transfer analysis of the passive residual heat removal system in ROSA/AP600 experiments," *Nuclear Technology*, vol. 124, no. 1, pp. 18–30, 1998.

[11] F. P. Incropera and D. P. DeWitt, *Fundamentals of Heat and Mass Transfer*, John Wiley & Sons, New York, NY, USA, 5th edition, 2002.

[12] H. Nourbakhsh, W. Wang, H. Ray, and T. Kress, "Historical perspectives and insights on ACRS review of AP1000 design certification," in *Proceedings of the 21st International Conference on Nuclear Engineering (ICONE '13)*, vol. 3, Chengdu, China, August 2013.

[13] X.-X. Pan, "Numerical study and sensitivity analysis of PRHR HX transient heat transfer performance," *Nuclear Power Engineering*, vol. 31, no. 1, pp. 97–102, 2010.

[14] R. J. Xue, C. C. Deng, and M. J. Peng, "Numerical simulation reaserch of natural convection heat exchanger," in *Proceedings of the Asia-Pacific Power and Energy Engineering Conference (APPEEC '10)*, pp. 1–5, IEEE, Chengdu, China, March 2010.

[15] Y. Li, C. Q. Yan, Z. N. Sun, and L. C. Sun, "Pool boiling heat transfer enhancement on porous surface tube," *Nuclear Science and Techniques*, vol. 22, no. 2, pp. 122–128, 2011.

[16] B. Jia, J. Jing, X. Qiao, and C. Zhang, "Numerical simulation of PRHR system based on CFD," *Journal of Applied Mathematics and Physics*, vol. 1, no. 6, pp. 74–81, 2013.

[17] H. Xia, D. Lu, Z. Du et al., "Thermal hydraulics numerical simulation and optimized design of passive residual heat removal heat exchanger in AP1000," in *Proceedings of the 21st International Conference on Nuclear Engineering (ICONE '13)*, Nuclear Engineering Division, Chengdu, China, August 2013.

[18] W. Zhang, W. Tian, S. Qiu, and G. Su, "Numerical investigation on heat removal capacity of passive residual heat removal heat exchanger," in *Proceedings of the 22nd International Conference on Nuclear Engineering (ICONE '14)*, vol. 4, Prague, Czech Republic, July 2014.

[19] Q. Men, X. Wang, X. Zhou, and X. Meng, "Calculation method of passive residual heat removal heat exchanger and numerical simulation," *Journal of Power and Energy Engineering*, vol. 2, no. 9, pp. 8–14, 2014.

[20] Y. Zhang, D. Lu, Z. Du, X. Fu, and G. Wu, "Numerical and experimental investigation on the transient heat transfer characteristics of C-shape rod bundles used in Passive Residual Heat Removal Heat Exchangers," *Annals of Nuclear Energy*, vol. 83, pp. 147–160, 2015.

[21] Q. Men, X. Wang, X. Zhou, and X. Meng, "Heat transfer analysis of passive residual heat removal heat exchanger under natural convection condition in tank," *Science and Technology of Nuclear Installations*, vol. 2014, Article ID 279791, 8 pages, 2014.

[22] M. Wang, W. Chen, and Y.-S. Lv, "Research on optimal design of passive residual heat removal heat exchanger," *Atomic Energy Science and Technology*, vol. 49, no. 3, pp. 455–459, 2015.

[23] W.-Q. Li, M.-F. Zhao, M.-H. Duan, Y.-Z. Chen, and H. Wang, "Numerical simulation on heat transfer experiment of passive residual heat removal heat exchanger at subcooled condition," *Yuanzineng Kexue Jishu/Atomic Energy Science and Technology*, vol. 50, no. 8, pp. 1410–1415, 2016.

[24] D. G. Lu, Y. H. Zhang, X. L. Fu, Z. Y. Wang, Q. Cao, and Y. H. Yang, "Experimental investigation on natural convection heat transfer characteristics of C-shape heating rods bundle used in PRHR HX," *Annals of Nuclear Energy*, vol. 98, pp. 226–238, 2016.

[25] T. Huang, Y. P. Zhang, H. Gong, W. X. Tian, G. H. Su, and S. Z. Qiu, "Development of the analysis tool for the water cooling type passive residual heat removal system of Chinese pressurized reactor," *Progress in Nuclear Energy*, vol. 90, pp. 164–174, 2016.

[26] R. B. Abernethy and J. W. Thompson, *Handbook Uncertainty in Gas Turbine Measurements*, Arnold Engineering Development Center, Arnold Air Force Station, Manchester, Tenn, USA, 1973.

[27] W. M. Rohsenow and H. Y. Choi, *Heat, Mass, and Momentum Transfer*, Prentice-Hall, Englewood Cliffs, NJ, USA, 1961.

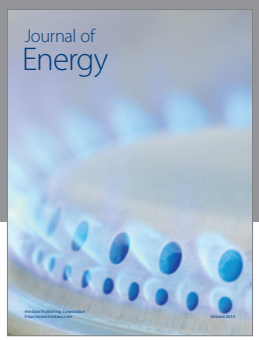

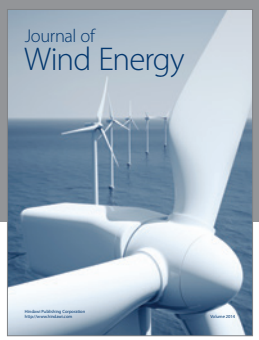

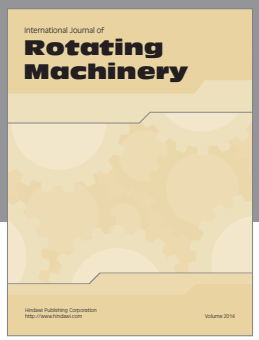

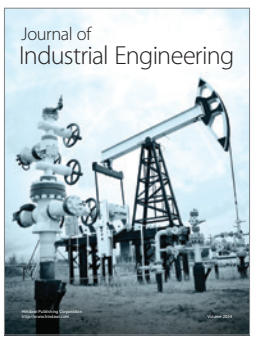

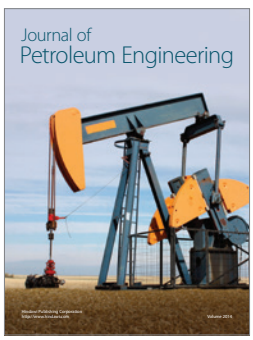

Hindawi
Submit your manuscripts at
https://www.hindawi.com